A CFD Model for Mass Transfer and Interfacial Phenomena on Single Droplets

Sylvia Burghoff and Eugeny Y. Kenig
Dept. of Biochemical and Chemical Engineering, University of Dortmund, 44221 Dortmund, Germany

DOI 10.1002/aic.11038
Published online November 3, 2006 in Wiley InterScience (www.interscience.wiley.com).

Mass transfer and interfacial phenomena during simultaneous extraction of two components from a single spherical droplet to a surrounding continuous phase were investigated both experimentally and theoretically. The experiments were carried out in a single droplet measuring cell in which the mass transfer of acetone and methylisopropylketone from the disperse toluene phase to the continuous aqueous phase was investigated. The developed model takes into consideration the cross-effects of multicomponent mass transfer and the onset of Marangoni convection induced by mass transfer. The influence of Marangoni convection on the velocity field around the droplet was analyzed. The developed model was implemented into the commercial computational fluid dynamics software package CFX4.3. The results of the performed simulations agree well with experimental data. Influences of Reynolds numbers of the continuous phase and initial mass fraction on the extraction process were analyzed. Furthermore, the effect of multicomponent mass transfer on the onset of Marangoni convection was studied. © 2006 American Institute of Chemical Engineers *AIChE J,* 52: 4071–4078, 2006
Keywords: CFD, multicomponent mass transfer, Marangoni convection, single droplet, measuring cell

Introduction

Liquid–liquid extraction represents an important and efficient method for numerous industrial applications. However, its basic phenomena are very complex and not yet fully understood. This lack of understanding makes the design of extraction units difficult and causes additional expensive pilot-plant experiments. The process understanding can be improved if the interdependencies are considered at the smallest representative scale. For most extraction operations, this scale is associated with a single droplet and its surface. Mass transfer of one or more components between the droplet and the surrounding phase, droplet size change arising from mass transfer, and the onset of Marangoni convection—all these interdependent phenomena have significant influence on extraction processes.

In multicomponent liquid systems, the direct proportionality between the transport of each individual component and its driving force (expressed either by concentration or by chemical potential gradient) is no longer valid. This brings about various cross-effects (osmotic diffusion, diffusion barrier, etc.) and makes the process behavior qualitatively more complex than that in binary systems.[1] The notion *Marangoni convection* generally encompasses phenomena caused by surface tension gradients at fluid interfaces. Marangoni convection may appear in many different forms, such as roll cells, ripples, or eruptions.[2] They lead to enhanced mixing of fluid elements near the interface and thus may appreciably accelerate mass transfer.[2] The interaction between multicomponent mass transfer and Marangoni effects was analyzed by von Reden.[3] He found that in the investigated quaternary system,

Correspondence concerning this article should be addressed to E. Y. Kenig at e.kenig@bci.uni-dortmund.de.

more intense interfacial phenomena appeared than in ternary systems. Besides, the onset of Marangoni convection was observed at lower concentrations of the transferred components. An explanation for these observations was not given in von Reden.[3]

It is very difficult to experimentally investigate this complex interplay of phenomena and, thus, rigorous theoretical methods are necessary to understand and properly describe liquid–liquid extraction processes. In this respect, computational fluid dynamics (CFD)—allowing the numerical simulation of complex fluid flow patterns inside and outside single droplets—represents a powerful method for the description of transport and interfacial phenomena.

Mass transfer of one component from a single droplet to a continuous liquid phase was recently modeled,[4–6] however, none of these works considered phenomena in multicomponent mixtures. The present work aims at a detailed description of liquid–liquid extraction including multicomponent mass transfer at a single droplet and the effect of Marangoni convection. Three systems—two ternary and one quaternary—were the focus of this investigation. The ternary systems are toluene/acetone/water and toluene/methylisopropylketone (MIPK)/water. A toluene/acetone/MIPK/water mixture, which constitutes the quaternary system, was chosen because of the different solubilities of both transferring components in toluene and water. Multicomponent effects are usually more pronounced in such systems.[7] In earlier works,[3,7] in which another quaternary system—toluene/acetone/phenol/water—was studied, the authors found that in systems with similar transport behavior of both transferring components characteristic multicomponent effects could not be observed.

Single-drop experiments can be performed fairly well in a measuring cell based on a Venturi injector with a specially designed drop collector facility.[8–10] This construction allows for arbitrary variation of residence time as well as high reproducibility of the measured concentrations. In Steiner[11] a detailed overview of systems analyzed in a drop measuring cell is given. In von Reden[3] the simultaneous mass transfer of two components across the drop interface was examined for the first time.

Simplified empirical and analytical models for description of multicomponent mass transfer at single droplets are not able to mirror the complex phenomena at the liquid–liquid interface. Therefore, in this work a rigorous model is presented to account for both multicomponent mass transfer and Marangoni convection. The model equations were solved using the commercial CFD tool CFX 4.3 (ANSYS Inc.). To verify the accuracy of the developed model, mass-transfer experiments at single droplets were also carried out to provide experimental data for the model validation. Several simulation studies were performed with the validated model, which brought new insights into the interdependencies in liquid–liquid extraction processes.

Experimental

The setup for measuring mass transfer at single droplets basically consists of a droplet measuring cell, a dosing pump, a gear pump, and a thermostat to maintain constant temperature in the system (see Figure 1). From a tank, the continuous aqueous phase is pumped through the measuring cell. Toluene is pressed through a capillary into the measuring cell using the dosing pump. This pump is used both for creation and for removal of the droplet. The toluene droplets contain a predefined amount of acetone and MIPK. The mass transfer of both components is observed during the experiments. The generated toluene droplet rises in the cell and is collected in a funnel at its top end. The measuring cell contains a Venturi injector, so that a variation of the flow velocity of the continuous phase in this area is obtained.[12] In the Venturi injector, droplets of different sizes can be brought to hover in the cell as a result of the different flow velocities. By varying the residence times of the droplets in the cell it is possible to analyze the mass-transfer behavior of the transferring components. For this study, toluene droplets of 1.5 mm radius were examined. The collected droplets were analyzed using a gas chromatograph.

Model Formulation

The system studied consists of a droplet and a surrounding continuous liquid phase (Figure 2). The phenomena in this system are inherently of a dynamic nature. The interactions in this two-phase system are manifold. The velocity field in each phase influences mass-transfer phenomena. Diffusional interactions of different species result in a coupled system of mass-transfer equations that should be solved simultaneously. In addition, the variables of the two liquid phases are conjugated in a complex way at the droplet interface. Finally, the droplet changes its size as the result of mass transfer and, thus, a moving interphase boundary arises. For an accurate description of this extraction system, all these coupling effects should be properly taken into account. To reduce the complexity, in this work, we focus on a spherical droplet and investigate the onset and the early stage of the Marangoni convection. This allows adequate study of the influence of Marangoni phenomena in a two-dimensional formulation.

The model is formulated under the following assumptions:

- Newtonian fluids
- Incompressible flow
- Isothermal system
- No mass transfer of the two carrier fluids across the phase interface (mutual saturation)[13]
- Laminar flow of both phases
- Droplet holds the spherical form

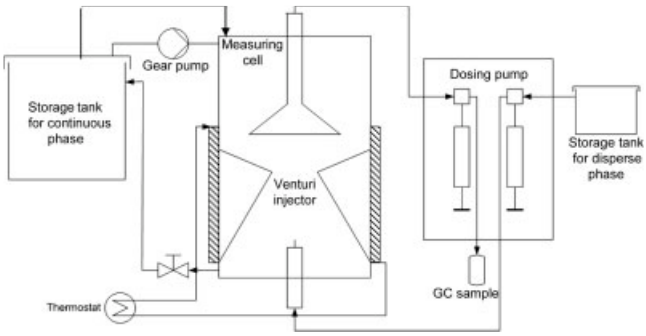

Figure 1. Experimental setup.

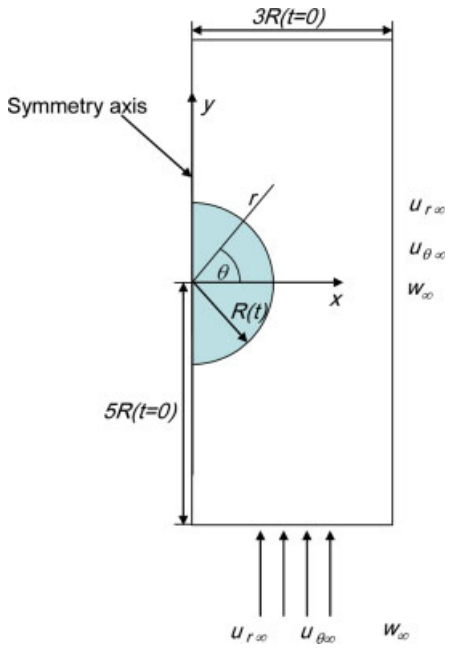

Figure 2. Axisymmetric model geometry of the droplet system.

[Color figure can be viewed in the online issue, which is available at www.interscience.wiley.com.]

- Absence of surface active contaminants
- No chemical reactions in the system

The process can then be described by the following equations.

Model equations for each phase

Continuity and Momentum Equations

$$\nabla \cdot \mathbf{u} = 0 \tag{1}$$

$$\rho\left[\frac{\partial \mathbf{u}}{\partial t} + \mathbf{u}\cdot\nabla\mathbf{u}\right] = -\nabla p + \mu\Delta\mathbf{u} \tag{2}$$

Mass-transfer Equation for a Multicomponent System

$$\frac{\partial(\mathbf{w})}{\partial t} + \mathbf{u}\cdot\nabla(\mathbf{w}) = \nabla\{[\mathbf{D}]\nabla(\mathbf{w})\} \tag{3}$$

Initial conditions at $t = 0$

System Velocity

$$\mathbf{u} = \mathbf{u}_p = 0 \tag{4}$$

Mass Fractions

$$(\mathbf{w})_p = (\mathbf{w}_0)_p = (\mathbf{w}_\infty)_p \tag{5}$$

$$(\mathbf{w}) = (\mathbf{w}_0) = (\mathbf{w}_\infty) \tag{6}$$

Boundary conditions at the system inlet (see Figure 2)

$$\mathbf{u} = \mathbf{u}_{in} = \mathbf{u}_\infty \qquad \text{at } r = -\frac{5R(t=0)}{\sin\theta} \tag{7}$$

$$(\mathbf{w}) = (\mathbf{w}_{in}) = (\mathbf{w}_\infty) \qquad \text{at } r = -\frac{5R(t=0)}{\sin\theta} \tag{8}$$

In Eqs. 7 and 8, an assumption of infinitely extended continuous phase is used.[14]

Boundary conditions far away from the droplet

$$\mathbf{u} = \mathbf{u}_\infty \qquad \text{at } r \to \infty \tag{9}$$

$$(\mathbf{w}) = (\mathbf{w}_\infty) \qquad \text{at } r \to \infty \tag{10}$$

Boundary conditions at the symmetry axis

$$u_\theta = \frac{\partial u_r}{\partial\theta} = u_{\theta,p} = \left(\frac{\partial u_r}{\partial\theta}\right)_p = 0 \qquad \text{at } \theta = \pm\frac{\pi}{2} \tag{11}$$

These conditions follow from the assumed droplet geometry.[14]

$$\frac{\partial(\mathbf{w})}{\partial\theta} = \frac{\partial(\mathbf{w})_p}{\partial\theta} = 0 \qquad \text{at } \theta = \pm\frac{\pi}{2} \tag{12}$$

Moreover, concentrations and velocities as well as their derivatives assume finite values at the center of the droplet[14]:

$$\mathbf{u},\ \frac{\partial\mathbf{u}}{\partial r},\ (\mathbf{w}),\ \frac{\partial(\mathbf{w})_p}{\partial r} \qquad \text{are limited at } r = 0 \tag{13}$$

The latter condition is set to avoid infinite values for the radial gradients at $r \to 0$ in the axisymmetric geometry.

Boundary conditions at the droplet surface[14]

Normal and Tangential Stresses

$$\left(p - 2\mu\frac{\partial u_r}{\partial r}\right)_p - \left(p - 2\mu\frac{\partial u_r}{\partial r}\right) = \frac{2\sigma}{R(t)} \qquad \text{at } r = R(t) \tag{14}$$

$$\mu_p\left[r\frac{\partial}{\partial r}\left(\frac{u_\theta}{r}\right) + \frac{1}{r}\frac{\partial u_r}{\partial\theta}\right]_p - \mu\left[r\frac{\partial}{\partial r}\left(\frac{u_\theta}{r}\right) + \frac{1}{r}\frac{\partial u_r}{\partial\theta}\right] = \frac{1}{R(t)}\frac{d\sigma}{d\theta} \qquad \text{at } r = R(t) \tag{15}$$

Continuity of Normal and Tangential Velocity Components[14]

$$u_{r,p} = u_r \quad \text{at } r = R(t) \tag{16}$$

$$u_{\theta,p} = u_\theta \quad \text{at } r = R(t) \tag{17}$$

Thermodynamic Equilibrium[1]

$$(\mathbf{w})_p = [\mathbf{M}](\mathbf{w}) \qquad \text{at } r = R(t) \tag{18}$$

where $[\mathbf{M}]$ is the matrix of distribution coefficients.

Continuity of Component Fluxes[1]

$$[\mathbf{D}_p]\frac{\partial(\mathbf{w})_p}{\partial r} + (\mathbf{w})_p \cdot \mathbf{u}_p = [\mathbf{D}]\frac{\partial(\mathbf{w})}{\partial r} + (\mathbf{w}) \cdot \mathbf{u} \qquad \text{at } r = R(t) \tag{19}$$

Transient change of the droplet radius

$$R(t+\Delta t) = \sqrt{R^3(t) - \frac{3\Delta t}{4\pi}\sum_{i=1}^{m}\left(\frac{M_i}{\rho_i}\int_A (J_i)dA\right)} \tag{20}$$

The latter condition is derived based on the assumption of spherical form of the droplet.

To account for Marangoni convection, the surface tension gradient resulting from the transport of acetone and MIPK was implemented in Eq. 15 using correlations obtained experimentally in Misek et al.[13] Because data for ternary systems only are available in the open literature, it was assumed that during multicomponent mass transfer the local surface tension gradient can be calculated as the sum of the gradients induced by individual species acetone and MIPK.

Model Implementation

The system of partial differential equations (Eqs. 1–3), together with initial and boundary conditions (Eqs. 4–20), cannot be solved analytically; instead, the system requires a numerical solution technique. The principle of computational fluid mechanics is based on the discretization of the derivatives of Navier–Stokes and mass-transfer equations with respect to time and space. In this work, the commercial CFD tool CFX4.3 is used for the model implementation. Given that a small spherical droplet surrounded by a laminar liquid flow was the focus of this study, the problem can be considered as axisymmetric.[14] With from this assumption, only the change of process variables with respect to the axis r and the angle θ should be considered, thus significantly reducing computational expense (Figure 2).

The droplet radius is set to 1.5 mm to match the experimental conditions described above. Moreover, for small droplets of this size, the spherical and axisymmetric shape of the droplet can still be assumed at Re = 400.[14] Density and viscosity of both the disperse and continuous phase depend on the concentrations of acetone and MIPK. Therefore, they are recalculated for each consecutive time step. The inlet velocity of the continuous phase varies from 10^{-6} to 10^{-1} m/s. The correlations for density, viscosity, and distribution coefficient as function of MIPK and acetone concentration are taken from Misek et al.[13] The UNIQUAC parameter values for the quaternary mixture are listed in Burghoff.[12]

In CFX 4.3, a liquid–liquid interface cannot be simulated using default program options. Therefore, the droplet surface is modeled using a standard boundary condition available in CFX 4.3, which is then modified by implementing the interfacial boundary conditions (Eqs. 14–19). This is done using Fortran subroutines. The system geometry is represented as seven blocks to enable reasonable meshing of the system with structured grids. For the grid generation, body-fitted grids are used to account for the spherical shape of the droplet. For numerical simulations, the geometrical system is meshed with 25,000 grid cells. Simulation tests performed with various grid cell numbers confirmed that this number guarantees stable simulation results independent of the number of cells.

The transient extraction process is calculated with a fully implicit backward-difference time-stepping procedure. The pressure–velocity coupling is modeled using the SIMPLE algorithm.[15] More detailed information on solution algorithms of the flow simulation can be found in the CFX4.3 manual.[16] For the calculation of implemented transient processes, such as droplet size change, the explicit Euler method was used. Implementation of Marangoni convection was achieved by use of the central difference scheme.

Process Analysis and Model Validation

Marangoni convection in ternary systems

If local surface tension gradients are induced at the phase interface, the velocity profiles change drastically as a result of the development of so-called roll cells at the interface. These roll cells can significantly enhance mass transfer by mixing of fluid elements close to the interface. Figure 3 shows the roll cells at the droplet interface for a system with Re = 0.004. Here, the mass transfer of acetone from a toluene droplet to a continuous aqueous phase is simulated.

This irregular velocity field has a direct influence on the concentration profiles of the transferring component in the droplet. The usual torus-like concentration profiles in systems with constant surface tension are completely destroyed and the droplet contents are subjected to intense mixing (see Figure 4).

At higher Reynolds numbers, the development of Marangoni convection is partly suppressed. This is obvious if the flow fields in Figure 5 and Figure 3 are compared. At the front side of the droplet, Marangoni convection cannot evolve because of the high velocity of the continuous phase, as any concentration gradient of the transferred component close to the interface, that could cause the development of roll cells, is instantaneously leveled out by the aqueous phase flow. At the rear side of the droplet, Marangoni convection still can develop because the velocity of the continuous phase is very small in this area. These different flow profiles at the front and rear parts of the interface induce separation of the continuous-phase flow from the droplet surface (Figure 5). As a result of this separation, a laminar vortex behind the droplet appears. This vortex cannot be established if the same system is considered neglecting Marangoni phenomena.

In a further simulation study, the influence of the Reynolds number of the continuous phase on the intensity of Marangoni convection and, consequently, on the rate of mass transfer was analyzed. Figure 6 shows the relative mass fractions of acetone w/w_0 against the Reynolds number of the continuous phase for both possible acetone transport directions. The w/w_0 values are calculated 10 s after the process start. For the mass transfer from the droplet to the continuous phase, the increasing velocity of the continuous phase in the system studied does not influence the relative mass fraction for Reynolds numbers $<$ 200. However, with a Reynolds number $>$ 200, a considerable enhancement of mass transfer can be observed because the interplay of Marangoni phenomena and flow convection in the continuous phase results in a very effective mixing of the droplet contents. For Reynolds numbers $>$ 300, no further significant enhancement can be recognized.

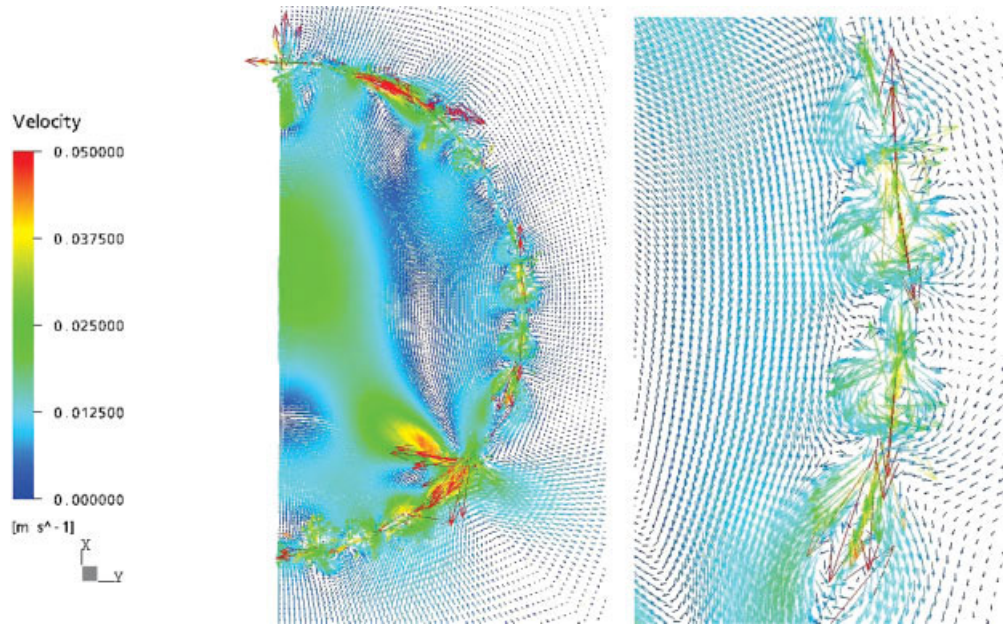

Figure 3. Marangoni convection (roll cells) at Re = 0.004.

Streamlines at half of the droplet (left); a larger view of a piece of the interface (right).

The situation is different for the mass-transfer direction from the continuous to the disperse phase. Here, the mass transfer is slowed down almost linearly with increasing Reynolds number of the continuous phase. With higher velocities of the continuous phase, fluid elements with strong concentration inhomogeneity are instantaneously replaced by fluid elements rich in the transferring component, so that the development of Marangoni convection is suppressed. Because of this suppression, the highest mass-transfer rate can be reached at high Reynolds numbers of the continuous phase, with the mass-transfer direction from the disperse to the continuous phase (see Figure 6).

Further analysis centered on the effect of the initial mass fraction of the transferring component on mass transfer using the toluene/acetone/water ternary system. The mass-transfer direction is chosen to be from the droplet to the aqueous phase, with a Reynolds number of the continuous phase of 0.004. Figure 7 shows the relative mass fractions 10 s after the process start against the initial mass fraction in the droplet. It is evident that the mass-transfer rate grows with higher initial mass fraction, if Marangoni convection is considered. In contrast, this rate remains constant, if the influence of Marangoni phenomena is neglected, that is, if the surface tension gradient in Eq. 15 is set to zero. The intensity of Marangoni convection increases with higher surface tension gradients and the latter grow when concentrations become higher. Therefore, high concentrations in the system lead to powerful interface phenomena and enhanced mass transfer.

Marangoni convection in a quaternary system

Simulation studies were also performed for the simultaneous mass transfer of acetone and MIPK, to analyze the interplay of multicomponent mass transfer and Marangoni phenomena. Figure 8 shows the concentration profiles of acetone and MIPK close to the droplet interface, after 2 s of transient mass transfer from the droplet to the continuous phase, neglecting the onset of Marangoni phenomena. It is obvious that the mass-transfer behavior of both components differs remarkably. Because of low solubility of MIPK in water resulting in a high distribution coefficient of about 10, its transport is much slower than that of acetone, with a distribution coefficient close to 1.

For the model validation, simultaneous mass transfer of both components, acetone and MIPK, from the droplet to the

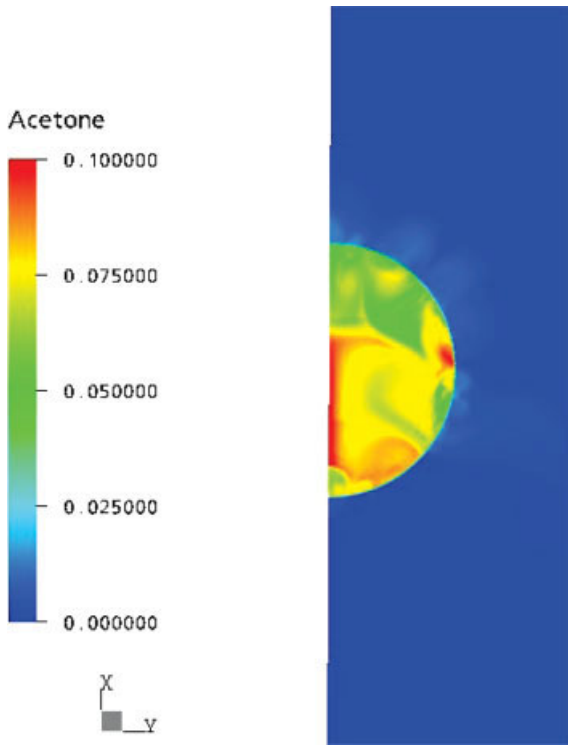

Figure 4. Concentration field of acetone at a single droplet at Re = 0.004.

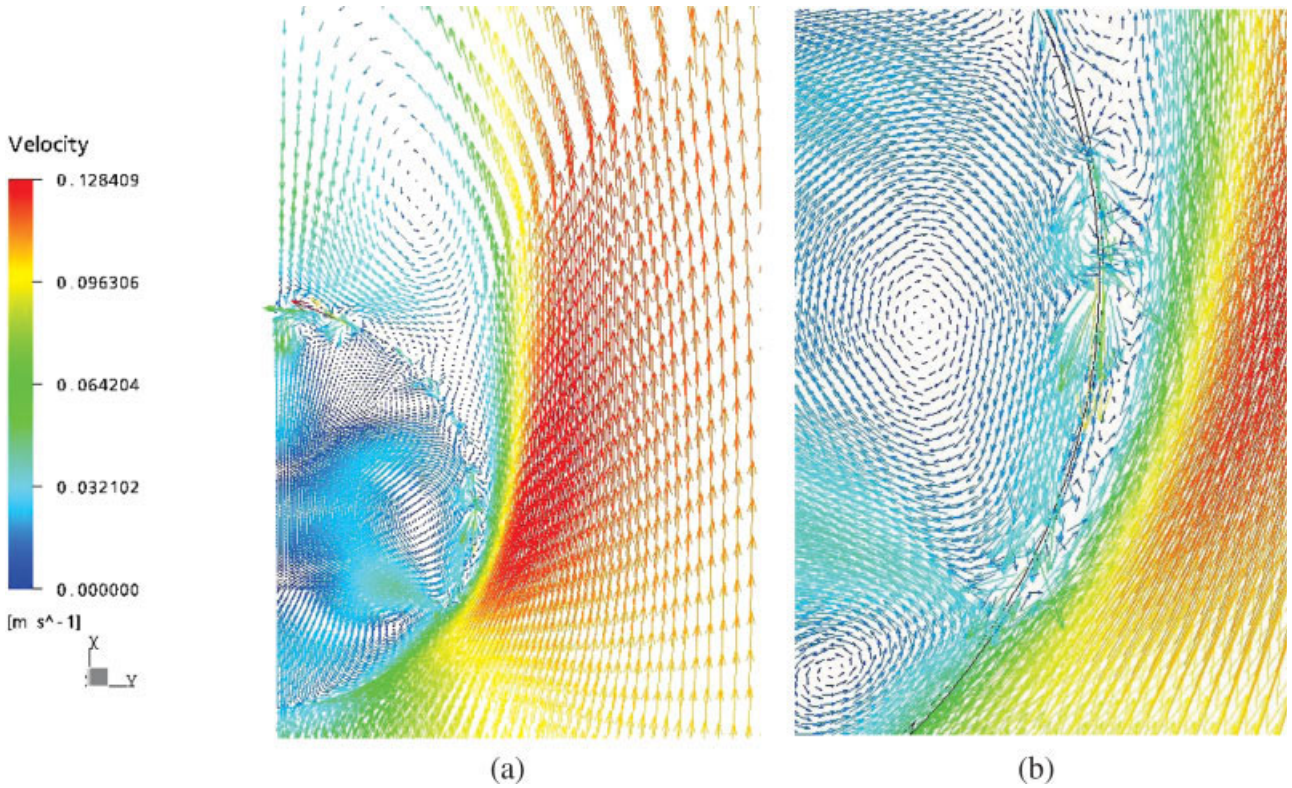

Figure 5. (a) Marangoni convection (roll cells) at Re = 400 (continuous phase): half of the droplet. (b) Marangoni convection (roll cells) at Re = 400 (continuous phase): a larger view of a piece of the interface (detail).

continuous phase was simulated including the Marangoni phenomena. The simulation results are compared with the experimental data (Figure 9). The error of the experimental data is estimated to 10% of the data point value. Generally, a good agreement is found. However, a certain systematic deviation is seen. This can be attributed to the overestimation of the surface tension gradient arising from the simplified assumptions. Additional experiments have to be performed to establish a better correlation for the surface tension gradient of multicomponent systems. As mentioned before, the simultaneous influence of two transferring components on the surface tension of the toluene/water two-phase system is not described in the literature and, therefore, the overall surface tension gradient caused by acetone and MIPK is set to the sum of the surface tension gradients induced by the individual components.

For further studies, mass transfer of one component from the droplet to the continuous phase is simulated, whereas another transferring component moves either in the same or in the opposite direction. Table 1 contains the relative mass fractions of the components for different mass-transfer scenarios. First, the mass transfer of acetone in the quaternary system was studied. If MIPK is also transferred from the droplet to the continuous phase, the mass transfer of acetone is enhanced compared to mass transfer in the ternary sys-

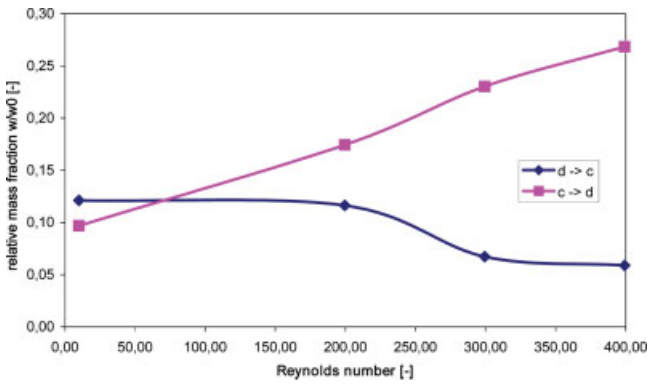

Figure 6. Influence of Reynolds number on mass transfer.

[Color figure can be viewed in the online issue, which is available at www.interscience.wiley.com.]

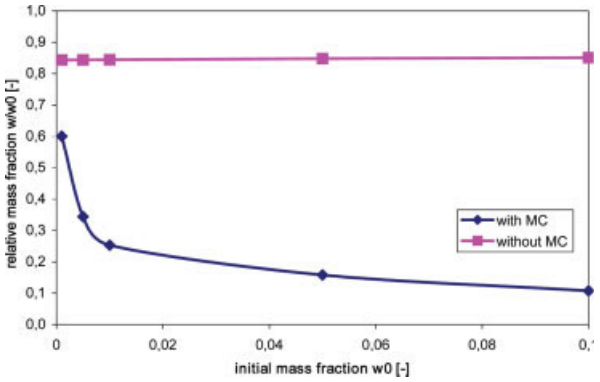

Figure 7. Influence of initial mass fraction on mass transfer.

[Color figure can be viewed in the online issue, which is available at www.interscience.wiley.com.]

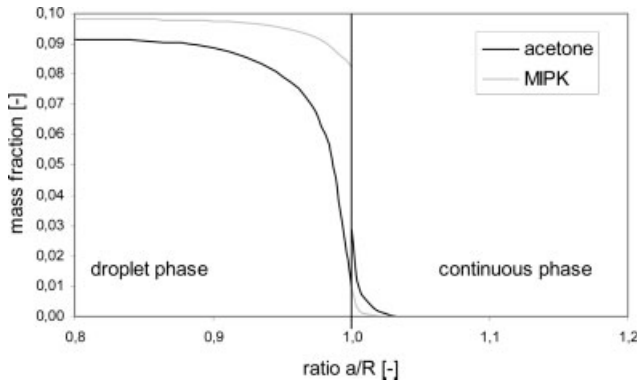

Figure 8. Concentration profiles of acetone and MIPK at the phase interface.

tem—the final mass fraction of acetone in the quaternary system is only one third of its mass fraction in the ternary system. When MIPK is transferred into the droplet from the continuous phase, the final mass fraction of acetone is even lower (11% of the final mass fraction in the ternary system). This unexpected phenomenon can be explained by the very high solubility of MIPK in toluene resulting in its rapid mass transfer into the droplet. The latter brings about stronger Marangoni convection at the interface and, consequently, an enhanced mass transfer of acetone to the continuous phase. On the contrary, the change in the mass fraction of MIPK is barely affected by acetone, for both directions of acetone transport. The reason is the low solubility of MIPK in water: in this type of mass-transfer process, the transition of MIPK across the interface is the slowest step, which cannot be accelerated by the convective transport of this component to the interface.

Further interaction effects

It was also interesting to study the influence of flow velocity on multicomponent mass transfer in a system with Marangoni phenomena. Figure 10 shows the difference of the relative mass fractions of acetone at Re = 0.4 and 400:

$$F = \left|\frac{w}{w_0}\right|_{\mathrm{Re}=0.4} - \left|\frac{w}{w_0}\right|_{\mathrm{Re}=400} \tag{21}$$

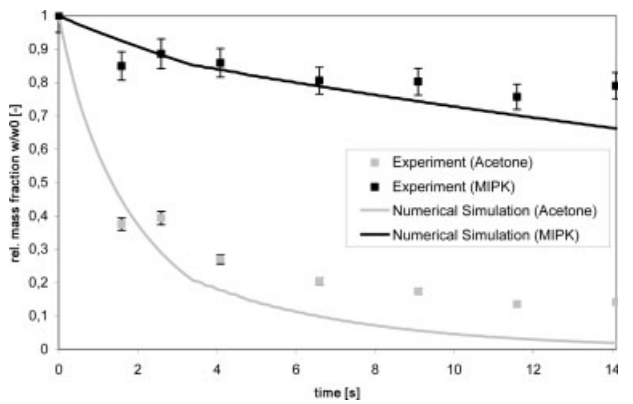

Figure 9. Relative mass fraction of acetone and MIPK in a toluene droplet (Re = 200).

Simulated and experimental data.

Table 1. Influence of Multicomponent Mass Transfer

Transport of	Conditions	Relative Mass Fraction, w/w_0
Acetone		
w_0 (acetone) = 0.01	Without MIPK	0.253
	With MIPK, same direction	0.083
	With MIPK, opposite direction	0.027
MIPK		
w_0 (MIPK) = 0.01	Without acetone	0.810
	With acetone, same direction	0.802
	With acetone, opposite direction	0.794

as a function of time. In the toluene/acetone/water ternary system, the mass fraction of acetone is always higher for Re = 400 than for Re = 0.4, that is, F is always > 0. This means that the mass transfer in the system with higher flow velocity always proceeds faster than the mass transfer in the system with lower velocity. On the contrary, in the quaternary system the mass fractions at Re = 400 are higher than those at Re = 0.4 at the beginning of the mass-transfer process. After some 6–11 s, this trend changes, and after 15 s the mass fractions of acetone are lower in the system with Re = 400.

The reason for this trend can be explained by the fact that in a quaternary system stronger Marangoni effects appear than those in a ternary system. At low flow velocities these phenomena can evolve without restrictions and show a strong influence on mass transfer. At high flow velocities, the onset of Marangoni convection is at least partly suppressed, as described above. This results in a slower mass transfer across the interface for high Reynolds numbers, compared to mass transfer in a system with Re = 0.4. As soon as the interfacial phenomena in the system with low velocity weaken, the mass fraction of acetone in the droplet becomes similar for both high and low flow velocities. The strong influence of high flow velocity in the droplet system leads to lower mass fractions in the droplet after 15 s at Re = 400, as compared to Re = 0.4. In Figure 10, the lines lie below the x-axis, if the influence of Marangoni phenomena in the system is stronger than that of the flow velocity; in the opposite case, the values of F are positive. We can see that multicomponent mass-transfer effects influence not only the mass-transfer behavior of the transferred components, but also the intensity of Marangoni

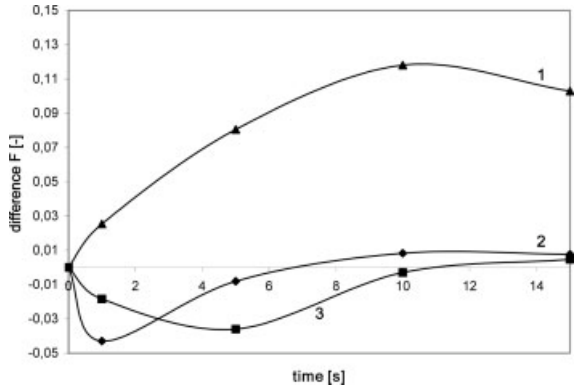

Figure 10. Time-dependent differences *F* of acetone: (1) without MIPK; (2) with MIPK in the same transfer direction; and (3) MIPK in the opposite transfer direction for Re = 400 and Re = 0.4.

convection in a given system. These results agree well with the experimental observations of von Reden.[3,12]

Conclusions

A rigorous model for the description of mass transfer and interfacial phenomena at single droplets in liquid–liquid extraction processes has been developed and implemented into the commercial CFD software CFX4.3 (ANSYS Inc.). The quaternary system toluene/acetone/MIPK (methylisopropylketone)/water is used for both theoretical and experimental analyses. Multicomponent mass transfer in the chosen system was modeled using the Maxwell–Stefan equations. Marangoni phenomena were accounted for in the numerical simulations, by implementing a term for calculation of the surface tension variation resulting from mass transfer. The onset of interfacial instabilities significantly changes flow conditions at the droplet. The droplet content is mixed intensely, resulting in enhanced mass transfer across the phase interface.

Along with the theoretical modeling, experiments at single droplets were carried out in a measuring cell for validation purposes and for testing the model quality. Especially for quaternary systems, experimental data for mass transfer are very rare in the literature. The simulation results were compared with the data obtained from experiments. The good agreement between simulation and experimental results proves the model predictivity.

In simulation studies, the influence of the flow velocity of the continuous phase on Marangoni convection was studied. With increasing Reynolds number of the aqueous phase, the onset of Marangoni phenomena is partially suppressed. At the front part of the droplet, concentration gradients cannot develop because fluid elements close to the interface are immediately swept away by the aqueous phase.

Further studies show that both mass-transfer direction and initial mass fractions of the transferring components have significant influence on the intensity of Marangoni phenomena. In multicomponent mass transfer, interfacial instabilities appear at lower initial mass fractions of the transferring components and are stronger than those in the corresponding ternary systems. These results agree with the experimental observations of von Reden.[3,12] Thus, the developed model is able to mirror the complex interacting phenomena at single droplets surrounded by a continuous phase and helps in understanding the interactions between multicomponent mass transfer, hydrodynamics, and interfacial phenomena in liquid–liquid extraction processes.

Acknowledgments

The authors gratefully acknowledge the financial support provided by DFG (German Research Foundation) Grant KE837/3.

Notation

A = area, m^2
a = distance from the interface, m
$(\mathbf{w})$ = vector of mass fractions, mol/m^3
$[\mathbf{D}]$ = matrix of diffusion coefficients, m^2/s
J_i = molar flux of component i, $mol/(m^2s)$
$[\mathbf{M}]$ = matrix of distribution coefficients
M_i = molar mass of component i, kg/mol
p = system pressure, $kg/(ms^2)$
R = droplet radius, m
Re = Reynolds number, $u_{in}3R(t = 0)/\mu$
r = cylindrical coordinate in radial direction, m
t = time, s
$\mathbf{u}$ = velocity vector, m/s
w = mass fraction

Greek letters

θ = cylindrical coordinate in circumferential direction, degree
μ = viscosity, m^2/s
ρ = density, kg/m^3
σ = surface tension, kg/s^2

Indices

0 = initial value at $t = 0$
i = component i
in = value at system inlet
p = disperse phase
r, θ = cylindrical coordinates

Literature Cited

1. Taylor R, Krishna R. *Multicomponent Mass Transfer*. New York: Wiley; 1993.
2. Sawistowski H. Grenzflächenphänomene. In: Hanson C, ed. *Neuere Fortschritte der Flüssig-flüssig-Extraktion*. Frankfurt am Main, Germany: Sauerländer; 1974.
3. von Reden C. *Multicomponent Mass Transfer in Liquid–Liquid Extraction*. Aachen, Germany: Shaker-Verlag GmbH; 1998.
4. Piarah WH, Paschedag A, Kraume M. Numerical simulation of mass transfer between a single drop and an ambient flow. *AIChE J*. 2001;47:1701–1704.
5. Waheed MA. *Fluiddynamik und Stoffaustausch bei freier und erzwungener Konvektion umströmter Tropfen*. Aachen, Germany: Shaker-Verlag GmbH; 2001.
6. Petera J, Weatherley LR. Modelling of mass transfer from falling droplets. *Chem Eng Sci*. 2001;56:4929–4947.
7. Brodkorb M. *Multicomponent and Contamination Effects in Liquid–Liquid Extraction*. Aachen, Germany: Shaker-Verlag GmbH; 1999.
8. Schröter J, Bäcker W, Hampe MJ. Stoffaustausch-Messungen an Einzeltropfen und an Tropfenschwärmen in einer Gegenstrom-Messzelle. *Chem-Ing-Tech*. 1998;70:279–283.
9. Henschke M, Pfennig A. Mass-transfer enhancement in single-drop experiments. *AIChE J*. 1999;45:2079–2086.
10. Schulze K, Paschedag A, Kraume M. Marangoni convection on liquid–liquid interfaces. 2nd International Berlin Workshop on Transport Phenomena with Moving Boundaries, Berlin; 2003.
11. Steiner L. Mass-transfer rates from single droplets and drop swarms. *Chem Eng Sci*. 1986;41:1979–1986.
12. Burghoff S. *Stofftransport- und Grenzflächenphänomene an Einzeltropfen in Flüssig-flüssig-Mehrkomponentensystemen*. Aachen, Germany: Shaker-Verlag GmbH; 2005.
13. Misek T, Berger R, Schröter J. *Standard Test Systems for Liquid Extraction Studies*. 2nd Edition. London, UK: The Institution of Chemical Engineers; 1985.
14. Clift R, Grace JR, Weber ME. *Bubbles, Drops, and Particles*. New York: Academic Press; 1978.
15. Patankar SV, Spalding DB. A calculation procedure for heat, mass and momentum transfer in three-dimensional parabolic flows. *Int J Heat Mass Transfer*. 1972;15:1787–1806.
16. ANSYS Inc. Product information CFX4.3. Canonsburg, PA: ANSYS; 2001.

Manuscript received Jan. 10, 2006, and revision Sept. 22, 2006.